Journal of Molecular Liquids 360 (2022) 119487

Contents lists available at ScienceDirect

Journal of Molecular Liquids

journal homepage: www.elsevier.com/locate/molliq

Evaluation of hydrogen storage ability of hydroquinone clathrates using molecular simulations

Trinidad Méndez-Morales [a,b,*], Hadrián Montes-Campos [b], Martín Pérez-Rodríguez [c], Manuel M. Piñeiro [a,*]

[a] CINBIO, Departamento de Física Aplicada, Facultade de Ciencias, Universidade de Vigo, E-36310 Vigo, Spain
[b] Grupo de Nanomateriais, Fotónica e Materia Branda, Departamento de Física de Partículas, Universidade de Santiago de Compostela, Campus Vida s/n, E-15782 Santiago de Compostela, Spain
[c] LFCR - ISABTP, Université de Pau et Pays de l'Adour, Allée du Parc Montaury, 64600 Anglet, France

ARTICLE INFO

Article history:
Received 14 January 2022
Revised 12 May 2022
Accepted 25 May 2022
Available online 29 May 2022

Keywords:
Hydrogen storage
Clathrate
Hydroquinone
Molecular simulations

ABSTRACT

Hydroquinone clathrates have been proposed as potential gas separation and storage media. Experimental results have demonstrated enhanced preferential adsorption for certain guest molecules, and also stability over temperature and pressure ranges that make them promising candidates to be employed in applications as hydrogen storage. Despite this, the characterization of these inclusion solids from thermodynamic and kinetic perspectives is still poor. In this work, we have tried to estimate the hydrogen storage ability of these clathrates using molecular simulations. The process of diffusion of hydrogen guest molecules from an external reservoir has been simulated using molecular dynamics, and the thermodynamic occupancy limit at different (T, p) conditions has been computed using hydrid Grand-Canonical Monte Carlo/Molecular Dynamics. The results show that hydrogen diffusion from an external reservoir is limited by interfacial phenomena in the clathrate surface, and also that multiple guest occupancy and its distribution can be computed using the described approach.

1. Introduction

In an era in which the energy sector is the source of most of greenhouse gas emissions, it is becoming clear that we need nothing less than a complete transformation of how we produce, transport and consume energy. Within this context, hydrogen is considered to be an alternative to face various critical energy challenges, since it offers ways to move towards the reduction of carbon in a wide range of sectors. It is already widely used in some industries, but it has not yet achieved its full potential to empower clean energy transitions. The implementation of hydrogen technologies is already receiving attention but its widespread use remains still challenging [1,2]. To make hydrogen an economically viable option several issues concerning its storage and release must be addressed, such as energy density, cost and total system mass.

In recent years, several research groups have considered nanostructured materials, such as zeolites, metal-organic frameworks and clathrates, for the storage of gases [3,4]. In particular, clathrates are nonstoichiometric inclusion compounds with a specific crystal structure containing holes (cages/cavities) of appropriate size inside the three-dimensional structure formed by bonding of atoms or molecules (hosts), in which other atoms or small molecules (guests) can be encapsulated (enclathrated) and move from one cage to another [5]. The term clathrate refers to both inorganic and organic hosts.

The family of inorganic clathrates in which hydrogen-bonded water is the host are more commonly known as hydrates [6]. Clathrate hydrates of small guests (such as hydrogen (H_2), argon (Ar), carbon dioxide (CO_2) or nitrogen (N_2)) [7–18] and of larger molecules (such as tetrahydrofuran (THF), methane (CH_4) or methyl iodide (CH_3I)) [19–21] have been extensively studied. However, storage applications of clathrate hydrates are very limited due to the rather extreme conditions of temperature and pressure necessary to their formation. This problem could be solved by using a promoter at the cost of reducing the storage capacity of the hydrate.

Concerning the organic molecules that can form clathrates, the hydroquinone (HQ) has been extensively studied and it was found to show some properties that can overcome the disadvantages of water when forming clathrates (such as vapor pressures due to water that can contaminate the purity of the separated gas phase when the hydrates are used for gas separation) [22]. Nevertheless,

* Corresponding author at: CINBIO, Departamento de Física Aplicada, Facultade de Ciencias, Universidade de Vigo, E-36310 Vigo, Spain (T. Méndez-Morales).
E-mail addresses: trinidad.mendez@usc.es (T. Méndez-Morales), mmpineiro@uvigo.es (M.M. Piñeiro).

https://doi.org/10.1016/j.molliq.2022.119487
0167-7322/

much of the research up to now concerns hydrates and very few practical applications were proposed for organic clathrates. HQ can crystallize into a solid substance that presents three different crystal structures: α, β, and γ, which need specific thermodynamic conditions to form [23]. The rhombohedral α-form is stable under ambient conditions and is able to accommodate small guests such as Ar, helium (He), xenon (Xe), N_2 and H_2 [24,25]. Since the α-form remains stable in the absence of guest molecules, this cannot be considered an enclathration phenomena but rather a solubilization of gas molecules. The metastable γ-structure can be obtained by sublimation or rapid evaporation of an ether solution of α-form. This form does not correspond to an inclusion compound [26].

Only the β-form is known to form clathrates in the presence of guest species under specific conditions of temperature and pressure [27–29]. Each HQ molecule takes part in the formation of two adjacent cavities. The β-HQ clathrate cages are limited at the top and bottom by planar hexagonal $[OH]_6$ rings, each of them resulting from the hydrogen bonding of the hydroxyl groups of six HQ molecules (Fig. 1.a) and with a radius of ~ 4 Å. In general, the β-HQ clathrate form is characterized by an stoichiometry factor of 3:1, that is, three HQ molecules per guest molecule; and an occupancy factor (the proportion of cages occupied by a guest) that goes from 0 (guest-free clathrate) to 1 (full clathrate with one guest per cage). However, Rozsa and Strobel observed multiple occupancy in H_2-loaded β-HQ clathrate at high pressure conditions [30].

A wide range of investigations of β-form HQ clathrate compounds were carried out. Among the numerous guest materials that have attracted attention we can find CH_4, N_2, Ar, carbon monoxide (CO), carbon dioxide (CO_2), oxygen (O_2), carbonyl sulfide (COS), hydrogen sulfide (H_2S), hydrogen fluoride (HF), acetonitrile (ACN), ethanol (EtOH), and methanol (MetOH) [31–51]. More recently, mixed-gas clathrates have also started to be considered with the purpose of selectivity/separation processes, mainly by Torré and coworkers [52–56] and Yoon and coworkers [57–64].

In this work we will focus on this β-structure containing H_2 as the guest molecule. Up to now, very few experimental works have analyzed the potential of these clathrate compounds as host media for recyclable and practicable storage of hydrogen [30,65,66]. For example, Yoon and coworkers [66] found that the storage capacity of the HQ clathrate highly depends on the loading pressure, ranging from a hydrogen weight percentage of 0.19 wt% at 10 MPa to 0.38 wt% at 35 MPa, both at room temperature. They also observed an extremely fast uptake and release of H_2 in the cages completed under 2 s. Moreover, Rozsa and Strobel[30] identified highly unusual behaviour of this system under high pressure (~ 3 GPa): multiple occupancy and negative compressibility.

On the other hand, computer simulations can provide us with detailed molecular-level information of these systems and complement details that are often difficult to characterize experimentally. For example, McGrail et al. [67] employed molecular dynamics (MD) simulations to study the molecular interactions and the dynamics of β-HQ clathrate loaded with different initial occupancies (from one to four) of H_2 per cage. They observed that higher loadings were stable at low temperatures (20 K), whereas at higher temperatures (300 K) greater displacement of hydrogen guests are favoured, which leads to lower loadings. More recently, Pérez-Rodríguez *et al.* [68] analyzed, by means of MD techniques and quantum mechanics calculations, the capture and release processes of the same host/guest pair. They reported the occurrence of spontaneous double occupancy per cavity and they concluded that β-HQ clathrate can be considered as a promising alternative to current strategies for H_2 storage. However, it must be noted that the capture process was modeled under stoichiometric conditions, that is, the number of H_2 gas molecules in the reservoir in contact with the empty HQ clathrate was equal to the number of cages inside the crystal.

Thus, we decided to analyze at the molecular scale the loading of the empty β-HQ clathrate in contact with a bulk of hydrogen whose density corresponds to the temperature and pressure conditions, which is more similar to the experimental procedure. For this purpose, we performed MD simulations that allowed us to understand the dynamic phenomena of capturing the gas molecules as well as the guest diffusion inside the crystal structure. In

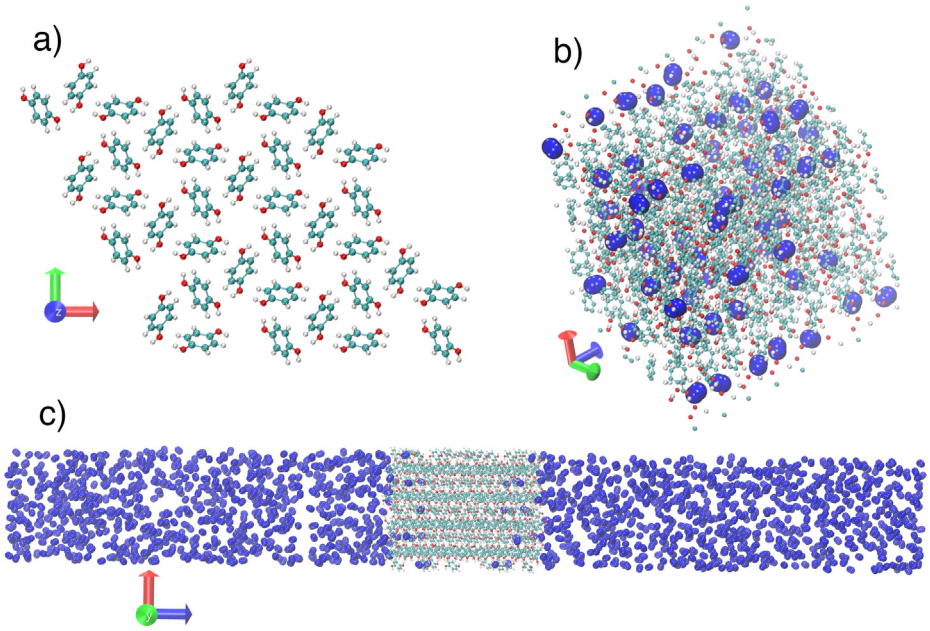

Fig. 1. (a) Cross section of the β-HQ clathrate structure, viewed along the z axis. Channels can be observed to be arranged in the z axis and delimited by the OH hexagons that are connected by H-bonds. There are 12 channels that correspond to 4 unit cells in the XY-plane. (b) Snapshot of the last frame in the hybrid GCMC/MD simulation at $T = 300$ K starting from a clathrate with no occupancy. (c) Schematic representation of the simulation box at the last step in the MD simulation at $T = 300$ K and $p = 400$ bar. Both in (b) and (c) the system is periodically repeated in the three directions. The relative size of hydrogen molecules (dark blue) has been increased for the purpose of clarity. Colour coding for the atoms of hydroquinone molecules is as follows: C, light blue; O, red; and H, white.

addition, hydrid Grand Canonical Monte Carlo/Molecular Dynamics (GCMC/MD) simulations were applied to determine the thermodynamic upper storage capacity limit of the HQ clathrate.

The outline of this paper is as follows. In Section 2, we provide a detailed account of the simulation method. In Section 3, we present and discuss the results obtained and concluding remarks are offered in Section 4.

2. Simulation details

2.1. Molecular dynamics simulations

MD simulations of HQ clathrates and hydrogen were performed using the GROMACS 2020.4 software [69–71] with the OPLS-AA force field [72], which includes both intramolecular (bond stretching, dihedral torsion and angle bending) and intermolecular forces (a van der Waals and a Coulomb term). Analysis and post-processing of the MD trajectories were done by using the standard GROMACS tools or coding an specific script in Python 3.9.1 with the library MDAnalysis [73,74].

The initial coordinates of the rhombohedral β-HQ clathrate were taken from experimental crystallographic data provided by Torré et al. [31] with CO_2 as molecule guest, the unit cell having the following dimensions: $a = b = (16.207 \pm 0.006)$ Å; $c = (5.780 \pm 0.002)$ Å. Then, $2 \times 2 \times 8$ replicated unit cells provided us with the crystalline structure used in the simulations, which contains of 288 hydroquinone molecules and consists of 12 channels with 8 cages per channel, as can be seen in Fig. 1. Concerning the force field used for the hydroquinone molecular model, the dispersive and intramolecular characteristic parameters used were those of OPLS-AA [75], combined with the partial atomic charges recalculated by Comesaña *et al.* [40]. This molecular model has been shown to describe with accuracy the structure of the hydroquinone β-clathrates for different pure guest molecules, and also for mixture clathrates [56]. For the case of the H_2, the model consists of two charged regular atoms constrained with a rigid bond and having a charge of $+0.4932e$, and by a charged virtual Lennard-Jones (LJ) site ($\sigma = 3.038$ Å and $\epsilon = 0.2852$ kJ/mol) located in the center of the molecule at 37.07 pm from each regular atom nucleus and carrying a charge of $-0.9864e$. The inclusion of the virtual atom aims at describing the quadrupole moment of the molecule [68]. All the molecules were considered to be nonpolarizable.

For modelling the capture process with MD, the simulation box was built by adding a bulk of hydrogen to the HQ system along the Z-dimension, that is, along the direction of the clathrate channels (Fig. 1.c). This bulk of H_2 is created with PACKMOL [76] by randomly placing inside of a box ~ 6 times greater than the clathrate structure the number of hydrogen molecules necessary to match the gas density at the pressure and temperature conditions of the simulation. Then, periodic boundary conditions were applied in all directions. Long-range electrostatic interactions were treated by using the Particle Mesh Ewald (PME) [77] method with a grid spacing of 12 nm and cubic interpolation. A cut-off distance of 1.1 nm was used for both Coulomb and LJ interactions. The geometric average was used for the combination rules of both LJ parameters [78]. The Linear Constraint Solver (LINCS) algorithm [79,80], with a fourth-order expansion of the constraint coupling matrix was used to fix all the bond lengths.

Initial configurations were relaxed during 10^6 steps using a conjugate gradient algorithm in order to remove bad contacts due to the initial random configuration of hydrogen molecules. The maximum step size and the tolerance were set to 0.01 nm and 0.1 kJ/(nm · mol), respectively.

Then, two different sets of simulations were performed in the isothermal-isobaric (*NpT*) ensemble, one of them corresponding to the isotherm $T = 300$ K and pressures of $p = (1, 10, 50, 100, 400, 500, 700)$ bar; and the other one corresponding to the isobar $p = 100$ bar and temperatures of $T = (150, 200, 250, 300, 350, 400)$ K, which are all of them below the dissociation temperature (~ 450 K) at this pressure. The temperature was kept constant by using the V-rescale thermostat introduced by Bussi et al. [81], with a coupling constant of 0.1 ps; whereas the pressure control was done by means of a semiisotropic Parrinello-Rahman [82,83] barostat, with a relaxation time of 1 ps. Compressibility in the X/Y-directions was set to the standard value of 4.5×10^{-5} bar^{-1}, but in the Z-direction this value was increased up to 10×10^{-5} bar^{-1} to take into account the rhombohedral symmetry of the clathrate crystal and the different response to variations of the pressure observed in the direction perpendicular to the gas-clathrate interface by Rozsa *et al.* [30].

For each simulation, the system was allowed to equilibrate during 20 ns, which was observed to be enough for properties such as the adsorption capacity to reach an equilibrium value. The resultant configurations were taken as the initial configurations for the production runs of 30 ns. The time step of the simulations was 1 fs. These *NpT* simulations were used to study the occupancy of the HQ-clathrate. Then, the final configurations were used as the initial configurations of 30 ns-long simulations in the *NVT* ensemble, in order to avoid the barostat having some impact on the calculation of the transport properties, such as the Mean Square Displacements (MSDs). Additional runs of 100 ps in which the velocities were saved at each step were carried out for the calculations of the Velocity Autocorrelation Functions (VACFs).

2.2. Hydrid grand canonical Monte Carlo/molecular dynamics simulations

Hybrid GCMC/MD simulations of H_2 uptake were carried out using the LAMMPS package [84]. This method is widely used in the study of gas adsorption in microporous materials [14,85–87] and, since the accommodation of guest molecules can be considered as an adsorption of the guest in the cages, it allowed us to account for hydrogen gas content of the clathrate at fixed volume, temperature and chemical potential of the guest species, μ. The number of adsorbates is changed to keep constant the chemical potential of the gas phase, which is identical to that of the guest molecules and is computed from the pressure of the bulk fluid.

The geometry and the force field parameters of the host are the same as those previously mentioned, whereas hydrogen was parameterized by using the Cracknell model [88]. In this case, the H_2 molecule is modelled as a rigid LJ dimer with parameters $\sigma = 2.59$ Å and $\epsilon/k_B = 12.5$ K. The bond distance between the two hydrogen atoms was 0.7414 Å and the force constant was set to be 374 kcal/(mol · Å^2). The specified bonds and angles are reset to their equilibrium values via the SHAKE algorithm [89]. A cutoff of 1.1 nm was used for both the LJ and Coulombic terms, and a long-range Van der Waals tail correction to the energy and pressure was added.

Two initial configurations were prepared in order to test the loading capacity of the β-HQ clathrate. The first periodic system consisted of the empty crystal structure (no occupancy), that is, only 288 HQ molecules; whereas in the second one each cage of the clathrate was loaded with identical configurations of three H_2 molecules (triple occupancy), that is, 288 HQ molecules and 288 H_2 molecules.

Each run in the μVT ensemble was performed at temperatures of 150 K and 300 K, which were kept constant by using the Nosé-Hoover thermostat [90] with a relaxation time of 10 fs. In all cases

the pressure of the gas reservoir was set to be 500 bar. The time step of the simulations was again 1 fs and each system was allowed to run for 400000 steps, that is, for 400 ps. No MC moves (translation/rotation) of a molecule were done and 10 GCMC exchanges (insertions or deletions, with equal probability) were attempted every 10 steps to control the number of guest molecules, which gives a total of 400000 trials. The insertion points are not limited to the centers of the cavities, but a guest hydrogen is allowed to be adsorbed at a random position in the available space inside the cages, even if they are already occupied by another guest molecule. The center of mass of the molecule is placed at the insertion point and the orientation of the guest is chosen at random by rotating around this point.

3. Results

3.1. H_2 adsorption in HQ-clathrates

In order to shed some light on the capture process, number densities (nm^{-3}) of H_2 molecules along the Z-direction were calculated from MD simulations and the profiles are shown in Fig. 2 for both the $p = 100$ bar isobar (Fig. 2a and c) and the $T = 300$ K isotherm (Figs. 2.b and 2.d). For these calculations, the positions of the hydrogen guests were computed by considering the virtual atom in the center of the molecule. The density profile for the clathrate structure is not completely shown since its height is much greater than that of the hydrogens, but it can be observed that the Z-coordinate is centered in the middle of the clathrate. In addition, in Fig. 2c and d vertical dashed lines have been included in order to delimit the cages inside the β-HQ clathrate. It must be noted that the position of the clathrate and the voids inside are approximated since only the data for one clathrate of the simulations was plotted, and due to the flexibility of the hydroquinone host lattice the cell volume can slightly change for different thermodynamic conditions [50].

We can observe that both in the isobar and the isotherm simulations there is a strong accumulation of H_2 molecules at the gas-clathrate interface. This accumulation of hydrogens increases with decreasing the temperature and with increasing the pressure, which is the same trend that follows the density of this gas. It

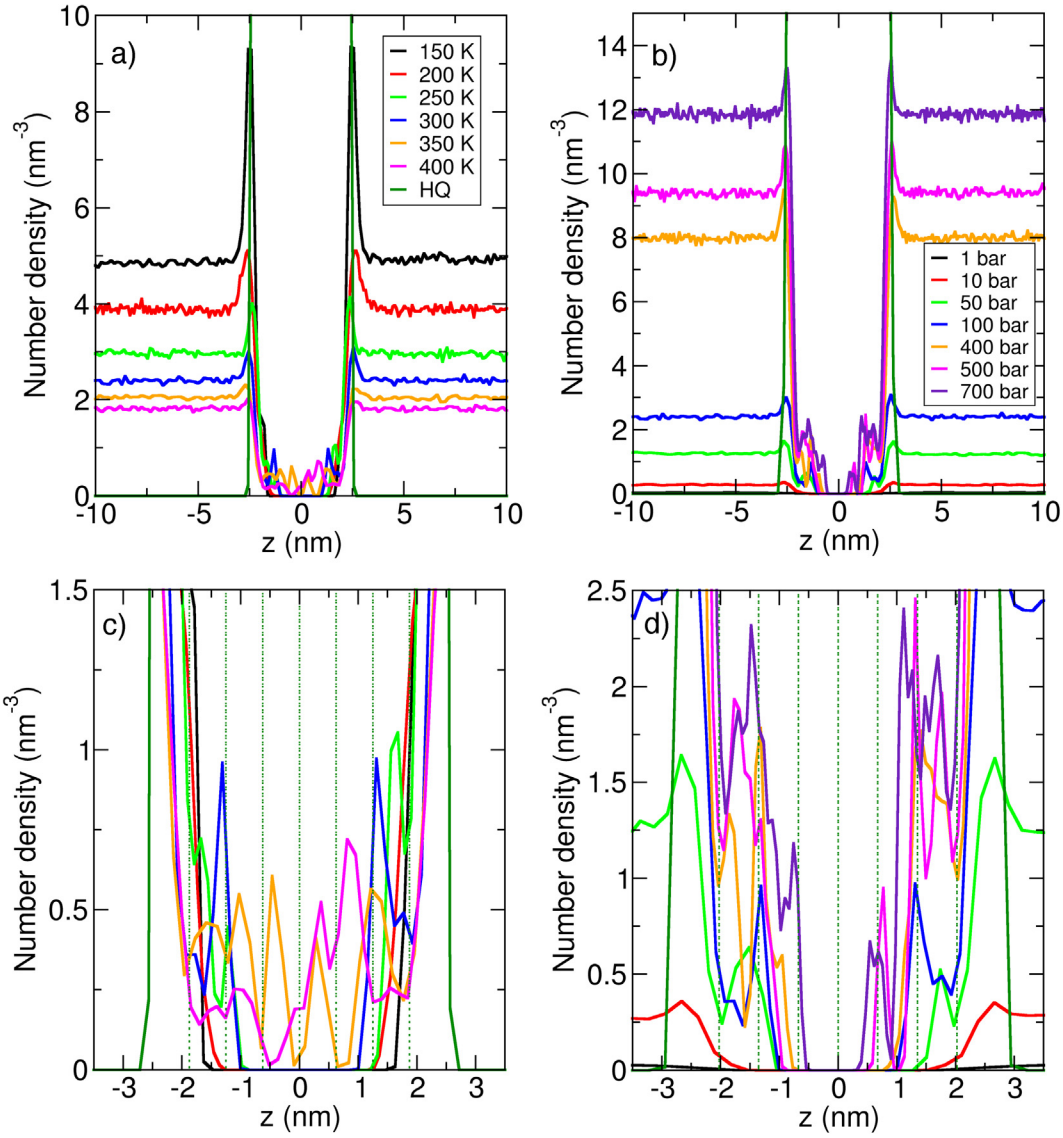

Fig. 2. Number density profiles (in nm^{-3}) in the Z-direction of the H_2 molecules in the vicinity and inside the clathrate channels for the (a) $p = 100$ bar isobar and the (b) $T = 300$ K isotherm from the MD simulations (the Z-coordinate is centered in the middle of the clathrate, named as HQ in the legend). (c) and (d) show a zoom of the inside of the clathrate in (a) and (b), respectively. Vertical dashed lines have been added with the purpose of showing the limits of the cavities along the channels in the Z-direction.

can also be seen that at $p = 100$ bar some of the guests are able to reach the center of the clathrate at the highest temperatures ($T = 350$ K and $T = 400$ K); whereas at $T = 300$ K no guests can diffuse into the innermost cages even at the highest pressures. That is, the ability of the β-HQ clathrate to allow for the entrance of the guests and their diffusion through the channels is not enough to accommodate the hydrogens at the rate they reach the interface. As a result, a dense layer of gas molecules is formed at the "entrance" of the clathrate that impedes the crystal structure to store a significant amount of hydrogen. Once the H_2 molecules are accommodated inside the clathrate and the interface is "blocked" they are no longer affected by the pressure of the bulk outside, which explains why the distance they are able to traverse in Fig. 2 does not vary with pressure as it does with the temperature. In addition, Pérez-Rodríguez et al. [68] stated that the barrier obtained from the potential energy for the transition of an H_2 guest from cage to cage through the hexagonal OH ring was around 100 meV for a hydrogen oriented parallel to the Z-axis, and it increased up to 120 meV for a perpendicular one. These values indicate a very low probability of intercage hopping and could explain the difficulties of the H_2 molecules to diffuse through the β-HQ clathrate channels and reaching the center of the structure.

In order to numerically estimate the occupancy of the β-HQ clathrate we computed the average number of hydrogens inside the structure by two different methods. In both cases a H_2 guest was considered to be enclathrated if the virtual atom in the center of the molecule satisfies the conditions imposed. The results are shown in Table 1 for all the MD simulations. In the first method (named as 10-oxygens in the table) we considered a hydrogen to be stored if it has at least 10 oxygen atoms closer than 6.4 Å. It must be noted that even though each cavity is delimited by two hexagonal $[OH]_6$ rings, it was too restrictive to impose having 12 oxygens within that distance. The second method (named as HQ limits in the table) consisted simply on considering the H_2 to be stored if its Z-coordinate is inside the interval defined by the highest and the lowest Z-coordinates of the clathrate.

It can be seen in Table 1 that increasing the temperature does not have a strong impact on the number of guests that are accommodated by the host, whereas this number increases significantly when increasing the pressure. We can deduce that varying the pressure has a stronger influence on the H_2 uptake, whereas modifying the temperature affects more the diffusion of the guest inside the crystal. Moreover, it is clear that the second method overestimates the occupancy since it takes into account some of the hydrogens that are located at the interface. Thus, the highest loading capacity was found at $T = 300$ K and $p = 700$ bar and it is shown to be around 0.22 wt% (100 × the ratio between the mass of absorbed hydrogen and the total mass of the system), which is clearly not enough for practical applications and quite lower than the value of 0.38 wt% observed by Yoon et al. [66] at the same temperature and $p = 350$ bar. If we consider a single occupancy of the cages we can conclude that only 36.5% of the cavities are occupied at these conditions.

Table 1
Average number of H_2 molecules inside the β-HQ clathrate channels during 30 ns of the MD simulations for the $p = 100$ bar isobar (up) and the $T = 300$ K isotherm (down). A single occupancy would correspond with 96 hydrogens inside the clathrate. In both cases two methods were compared for calculating the cage occupancy: (i) those hydrogens that have at least 10 oxygens closer than 6.4 Å are considered to be inside the clathrate ("10-oxygens" in the table), and (ii) those hydrogens whose z coordinates are within the interval defined by the smallest and the largest z values of the clathrate are considered to be inside it ("HQ limits" in the table).

AVERAGE OCCUPANCY MD p = 100 bar		
Temperature (K)	10-oxygens	HQ limits
150	6(2)	35(4)
200	6(2)	27(5)
250	7(2)	22(5)
300	7(2)	19(4)
350	10(3)	25(6)
400	10(2)	26(5)
T = 300 K		
Pressure (bar)	10-oxygens	HQ limits
1	0.0(1)	0.2(4)
10	0.3(6)	2(1)
50	3(2)	10(3)
100	7(2)	19(4)
400	21(2)	55(8)
500	23(4)	61(9)
700	35(4)	81(10)

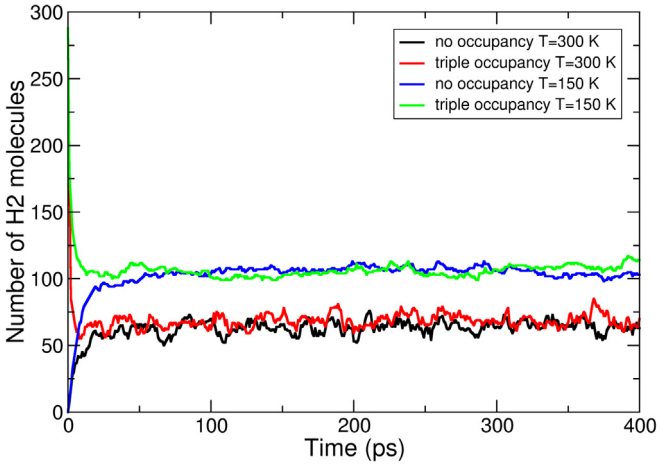

Fig. 3. Number of H_2 molecules inside the β-HQ clathrate as a function of time for the hybrid GCMC/MD simulations starting from different initial conditions: empty clathrate at $T = 150$ K (blue) and $T = 300$ K (black); and clathrate with triple guest occupancy at $T = 150$ K (green) and $T = 300$ K (red). In all cases the crystal structure is in contact with a a reservoir of H_2 gas at 500 bar.

On the other hand, the thermodynamic upper limit for the H_2 uptake capacity of the HQ clathrate was determined by means of hybrid GCMC/MD simulations, starting the simulations from two different initial configurations. The first one is an initial guest-free clathrate, and the second one starts from a fully loaded structure, with triple guest occupancy per cage. In Fig. 3 we show the estimation of the H_2 gas content of the clathrate as a function of time for two different temperatures, $T = 150$ K and $T = 300$ K (it must be remembered that the system is in equilibrium with a hydrogen reservoir whose pressure is 500 bar). In all cases, it can be observed that the curves showing the evolution of the number of enclathrated hydrogen molecules rapidly reach a plateau, and the equilibrium states are achieved by the initial 25 ps, that is, after approximately 25000 creation/deletion trials. Also, for a given temperature, the H_2 content converges to the same equilibrium value of guest molecules regardless the initial occupancy.

The average occupancy results for the last 200 ps of the hybrid GCMC/MD simulations are included in Table 2. Compared to some previous experimental results reported by Yoon and coworkers [66], who observed an H_2 content of 0.38 wt% at 35 MPa and room temperature; the hybrid GCMC/MD simulations show that these cavities could reach an occupancy rate of $\theta = 0.68$, that is, 0.41 wt% at the same temperature and slightly higher pressure. This is ~ 3 times greater than our previous estimation of 0.15 wt % obtained from MD simulations (Table 1). At $T = 150$ K the value of the adsorption plateau corresponds to a case where some of the cages are occupied by two H_2 molecules (single occupancy, $\theta = 1.0$,

would correspond with 96 hydrogens). However, at $T = 300$ K the analysis of the simulation box revealed that some the cavities also present double guest occupancy even though the whole crystal structure is at $\theta = 0.68$; but it must be noted that this is generally the case for less than 2% of the holes. In any case, these results evidence that multiple occupancy can be studied using the molecular modelling setup proposed, opening perspectives for further analysis.

3.2. Dynamics of H_2 inside HQ-clathrates

Single-particle dynamics in these systems was analyzed only for those guest molecules that were observed to be adsorbed during the 30 ns of the production *NVT* runs (or 100 ps for the VACFs). It must be noted that for the three lowest temperature of the isobar ($T = 150$ K, $T = 200$ K and $T = 250$ K) and the two lowest pressures of the isotherm ($p = 1$ bar and $p = 10$ bar) there were no hydrogens satisfying this condition. For the other systems the number of guests was found to be between 1 and 15 depending on the thermodynamic conditions of the simulation.

MD is a good method to investigate the hydrogen diffusion process inside the β-HQ clathrate channels through the calculation of the Mean Square Displacement (MSD), which is defined as

$$MSD = \langle \Delta|\vec{r}(t)|^2 \rangle = \frac{1}{N} \langle \sum_{i=1}^{N} |\vec{r}_i(t) - \vec{r}_i(0)|^2 \rangle, \quad (1)$$

where $\vec{r}(t)$ is the location of the center of mass of gas molecule i at time t, the sum extends over all the hydrogen molecules present in the clathrate and brackets indicate the ensemble average. Fig. 4 shows the log-log plot of MSD with time for the $p = 100$ bar isobar and the $T = 300$ K isotherm.

This plot can be divided into three regions: the first one, below approximately 1 ns, shows for most of the curves an anomalous diffusion with a slope close to zero; the second region, which corresponds to the central part of the plot, is a gradual transition to the third region, between $10 - 20$ ns, where hydrogen diffuses inside the clathrate. At long times the fluctuations in the curve increase due to decreasing statistics. In addition to the very slow diffusion revealed by this figure, we can observe that some of the curves show a shoulder in the intermediate region, which corre-

Table 2
Average number of H_2 molecules inside the HQ clathrate from hybrid GCMC/MD simulations at $T = 150$ K and $T = 300$ K, starting from two different configuration: an empty clathrate (up) and a clathrate with 3 hydrogen guests per cavity (down). In all cases the crystal structure is in contact with a a reservoir of H_2 gas at 500 bar.

AVERAGE OCCUPANCY GCMC/MD		
Occupancy	Temperature	
	150 K	300 K
None	106(3) (0.67 wt%)	65(4) (0.41 wt%)
Triple	107(3) (0.68 wt%)	69(5) (0.44 wt%)

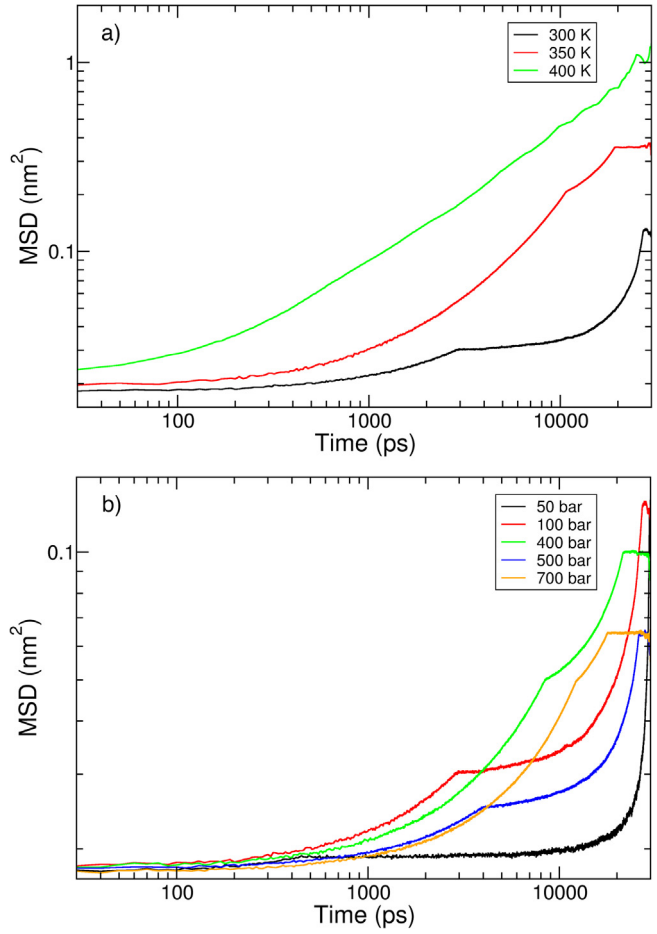

Fig. 4. Log-log plot of the time dependence of the MSDs of the H_2 molecule for those guests that were observed to be all the time inside the clathrate channels during 30 ns of the MD simulations for the $p = 100$ bar isobar (a) and the $T = 300$ K isotherm (b).

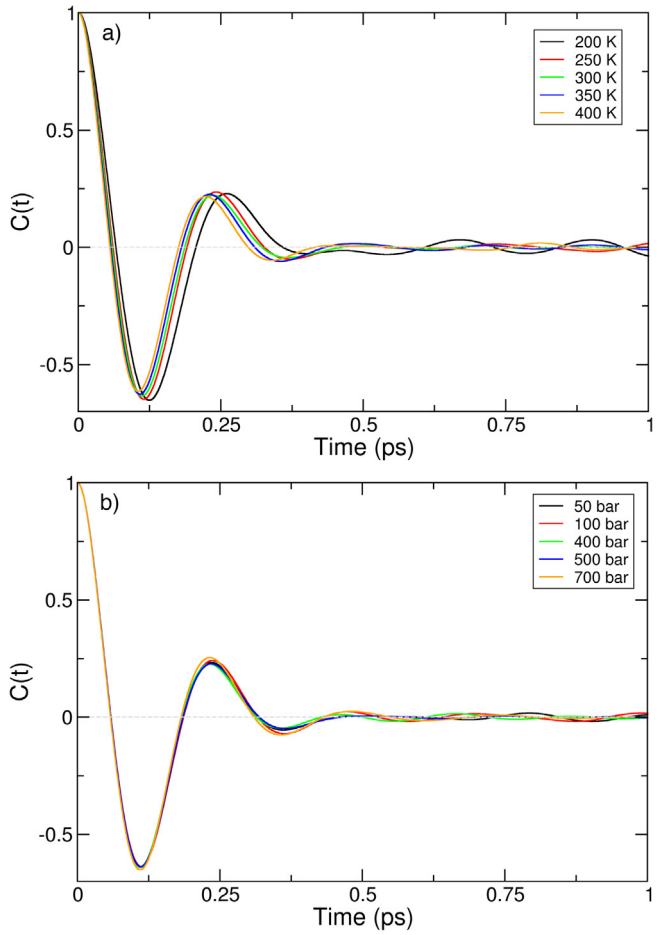

Fig. 5. VACFs of the H_2 molecule for those guests that were observed to be all the time inside the clathrate channels during 100 ps of the additional MD simulations for the $p = 100$ bar isobar (a) and the $T = 300$ K isotherm (b).

sponds to cage-to-cage hopping of H_2 guests. Moreover, the plot at constant pressure (Fig. 4.a) displays that H_2 molecules reach longer distances under these conditions than the set of simulations at constant temperature (Fig. 4.b). This is in good agreement with the results included in Fig. 2. At 100 bar, when the temperature increases the guests are able to travel around $0.7 - 0.9$ nm, that is, there are spontaneous hopping events of H_2 molecules across the neighboring cavities. However, at 300 K the guests do not traverse, on average, more than 0.4 nm regardless the pressure, which reveals that the movement of most of the H_2 molecules is confined inside the same clathrate cage. As stated in the previous section, once the hydrogens of the bulk are adsorbed by the HQ-clathrate they are not affected anymore by the pressure of the reservoir and the rate of diffusion is governed by the temperature.

One way of further understanding the dynamical properties is through the calculation of the center-of-mass Velocity Autocorrelation Functions (VACFs) of the guests. The normalized VACF is computed as

$$C(t) = \frac{\langle \vec{v}(t) \cdot \vec{v}(0) \rangle}{\langle \vec{v}(0) \cdot \vec{v}(0) \rangle}, \tag{2}$$

where $\vec{v}(t)$ is the velocity of the center-of-mass of the molecule at time t and the brackets indicate the ensemble average. In Fig. 5, the temperature and pressure dependence of dimensionless VACFs of H_2 molecules are shown for the $p = 100$ bar isobar and the $T = 300$ K isotherm.

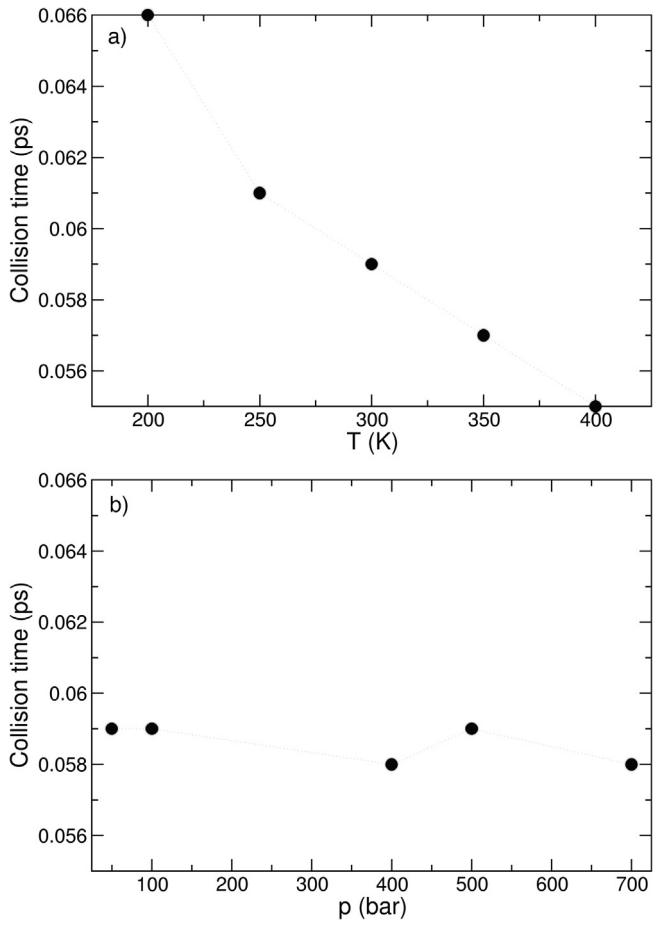

Fig. 6. Mean collision time of the H_2 molecule for those guests that were observed to be all the time inside the clathrate channels during 100 ps of the additional MD simulations for the $p = 100$ bar isobar (a) and the $T = 300$ K isotherm (b).

As it can be seen, the VACFs exhibit an oscillatory behaviour that is coherent with a rattling motion of the guests that are entrapped in the cages. In addition, all the VACFs decay in a subpicosecond scale, and the first zero of the curve, which is around 0.06 ps in all cases, indicates the mean collision time of hydrogen molecules. As it is shown in Fig. 6, this mean collision time slightly increases (from 0.055 ps to 0.066 ps) with decreasing the temperature but, once again, no effect of the pressure was registered on this magnitude.

In addition, the vibrational Density of States (vDOS) can be straightforwardly obtained, since it is directly related to the Fourier transform of the VACFs

$$I(\omega) = \int_0^\infty e^{-i\omega t} C(t) dt \tag{3}$$

We assume the convention here that $I(\omega)$ is normalized such that

$$\int_0^\infty I(\omega) d\omega = 1 \tag{4}$$

The results for the guest molecules are shown in Fig. 7. A broad band centered at about 130 cm^{-1} was predicted in all cases. Upon increasing the temperature the spectrum shows a slight shift to higher frequencies as a consequence of the increased thermal velocities of the small guests. However, no difference was noticed when varying the pressure, as expected.

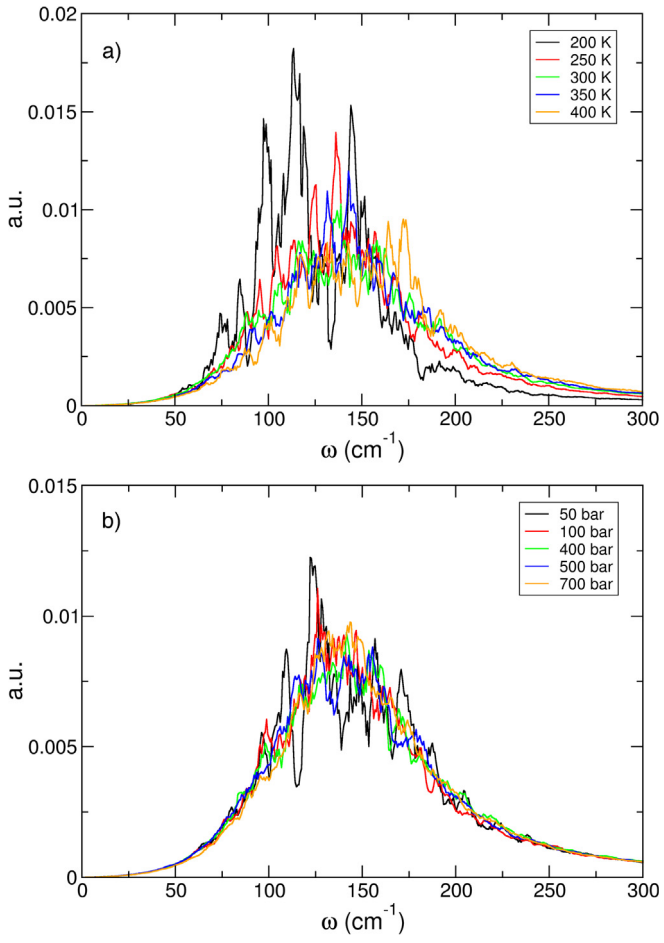

Fig. 7. vDOS of the H_2 molecule for those guests that were observed to be all the time inside the clathrate channels during 100 ps of the additional MD simulations for the $p = 100$ bar isobar (a) and the $T = 300$ K isotherm (b). The fluctuations were smoothed with a running average of length 7.

Finally, with the aim of obtaining a more complete statistical description of the dynamics properties plotted in Figs. 4 and 5 (MSDs and VACFs, respectively), we have performed multiple replications of the run at $T = 300$ K and $p = 700$ bar. The results are shown in Fig. 8.a and Fig. 8.b, from which a qualitative analysis of the uncertainties can be obtained and extrapolated to the other systems. It can be observed that the MSDs strongly depend on the occupancy of the clathrate and the moment at which the guests move from one cage to another. Since the number of enclathrated molecules is very low there is marked variability in the curves but it does exist a compatibility among them. On the other hand, VACFs do not differ from each other due to the lower characteristic time as compared to the intercage hopping and this movement being restricted to the volume of a cage. In addition, we considered an unidimensional model of the diffusion to obtain a better understanding of the MSDs. The model considers two different contributions to the movement of the atoms. The first one defines constant probability of jumping between cages, which act as jumps between adjacent clathrate cages. The mean time of the jump was set at 20 ns and its direction is randomly chosen. The second one is the vibration of the particles inside the cages. Due to the much smaller characteristic time of this movement, compared to the intercage one, the contribution of this movement to the MSD is a constant value and can be considered as independent of the jumping between cages. This value was set at 0.02 nm^2 by looking at the value of the simulated MSDs at small times. The results, included in Fig. 8.c, show the MSDs obtained with this model applied to systems with a different number of particles and it can be clearly seen that the behaviour of the MSDs obtained with GROMACS is well reproduced.

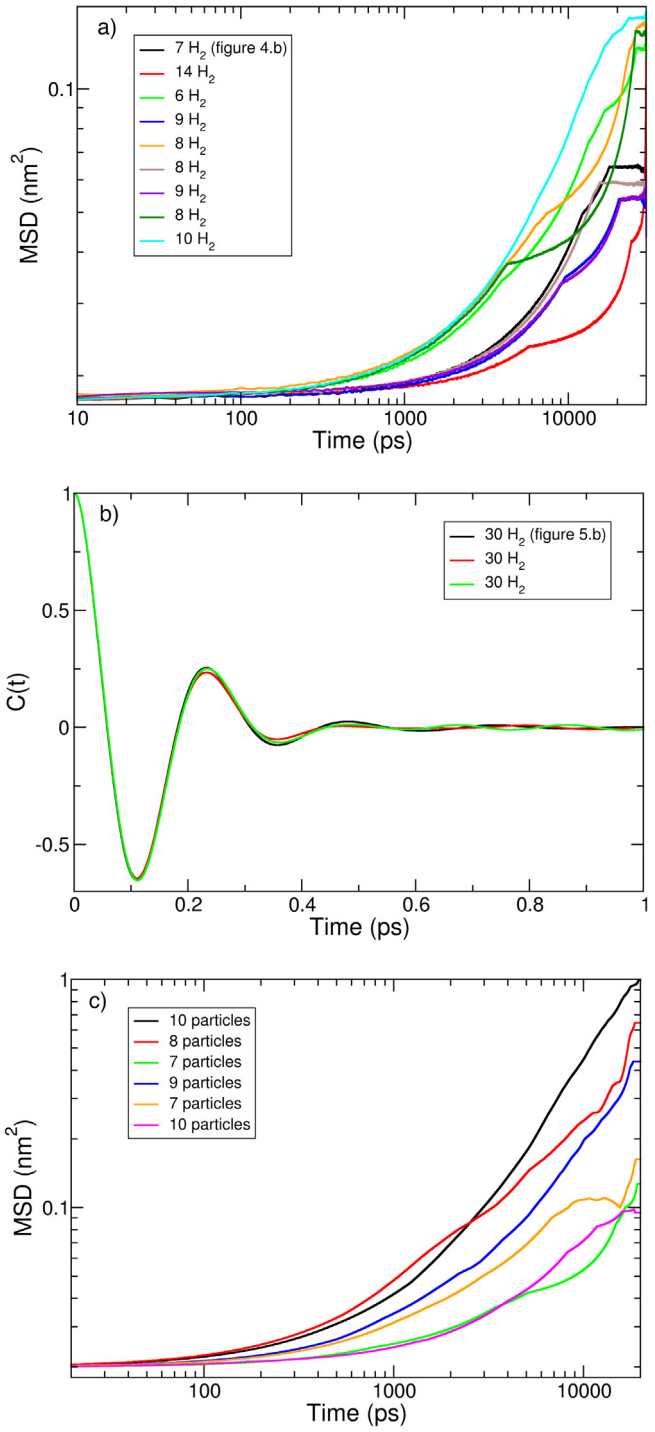

Fig. 8. MSDs (a) and VACFs (b) obtained from multiple replications of the simulation run at $p = 700$ bar and $T = 300$ K (including the data from Figs. 4 and 5). The legends show the number of hydrogens employed for the calculations, that is, those that are observed to be inside the clathrate during 30 ns and 100 ps, respectively. MSDs (c) from an unidimensional diffusion model applied to systems with different number of particles.

4. Conclusions

The potential use of hydroquinone clathrates as hydrogen storage media is conditioned by a number of factors not fully understood yet. One of them is the maximum storage capacity that may be obtained, a key factor to determine whether this option improves the efficiency of the already existing alternatives. The experimental and theoretical studies concerning this question are still scarce. Following previous works where the estimation of hydroquinone clathrates structure and equilibrium were analyzed using molecular dynamics, in this study we have tried to determine the maximum occupancy of the β-clathrate structure by hydrogen guest molecules.

The first setup tested considered the empty clathrate structure, in direct coexistence with a bulk of hydrogen. Calculations were performed for the isotherm of 300 K, in the pressure from 1 to 700 bar, and for the isobar of 100 bar in the 150 to 400 K range. The intention of this setup was twofold, trying to explore the dynamics of the filling process of an empty structure in contact with an external reservoir, resembling a possible real loading procedure, up to the maximum occupancy. The results of these tests were that the combination of slow diffusion of the guests through the solid and formation of a high density adsorbed hydrogen layer in the clathrate surface represented a limiting hindrance that completely blocked the loading process. The evolution of occupancy and surface adsorption has been discussed in these cases. The results of this test are very instructive and pose several key questions that have to be carefully considered from a practical point of view related to the filling-emptying cyclic process. The dynamics of the enclathrated guest molecules was analysed also through the study of mean square displacements, velocity autocorrelation functions, and density of states distribution.

As the previous option did not allow to determine the structural maximum occupancy, an alternative methodology was proposed. Hybrid Grand-Canonical Monte Carlo/Molecular Dynamics simulations were then performed, with the aim of overcoming the limitation of slow diffusion and clathrate channel entrance clogging observed in the previous calculations. Trying to determine the influence of the initial clathrate occupancy state on the final results, calculations were started in this case from two opposed initial setups, namely the empty structure, and an overloaded tri-

ple occupancy crystal. For every condition tested, both calculations starting from the described initial configurations converged to the same equilibrium occupancy rate. The occupancy determined following this technique matches closely experimentally reported values, which represents another remarkable validation for the molecular model used to describe both the host (hydroquinone) and guest (hydrogen) molecules. For the case of higher uptake, double occupation appears spontaneously, but combined with singly occupied and even empty cages. This means that this feature of guest multiple occupancy, essential for practical objectives, can be studied using the proposed technique, opening perspectives to more detailed analysis.

The results presented underline the validity of the molecular simulation approaches used in the quantitative determination of macroscopic storage capacities for this type of clathrates. In addition, the precise molecular scale description of the dynamics of the guest molecule diffusion process obtained has to be emphasized as a value of this calculations, as its detailed understanding and possible tuning is a key towards the development of feasible practical applications related with hydrogen storage.

Declaration of Competing Interest

The authors declare that they have no known competing financial interests or personal relationships that could have appeared to influence the work reported in this paper.

Acknowledgments

T. M.-M. thanks the Spanish Ministry of Science, Innovation and Universities for her Juan de la Cierva grant IJC2018-036774-I. The financial support of the Xunta de Galicia (GRC ED431C 2020/10 and GRC ED431C 2020/06) is gratefully acknowledged. M. P.-R. thanks the support of the Investissement d'Avenir French programme (ANR-16-IDEX-0002) under the framework of the E2S-UPPA hub Newpores. Facilities provided by the Galician Supercomputing Centre (CESGA) are also acknowledged.

References

[1] J. Andersson, S. Grönkvist, Large-scale storage of hydrogen, Int. J. Hydrog. Energy 44 (2019) 11901–11919.
[2] R. Moradi, K.M. Groth, Hydrogen storage and delivery: Review of the state of the art technologies and risk and reliability analysis, Int. J. Hydrog. Energy 44 (2019) 12254–12269.
[3] M. Hirscher, B. Panella, Hydrogen storage in metal–organic frameworks, Scr. Mater. 56 (2007) 809–812.
[4] J. Dong, X. Wang, H. Xu, Q. Zhao, J. Li, Hydrogen storage in several microporous zeolites, Int. J. Hydrog. Energy 32 (2007) 4998–5004.
[5] L. Mandelcorn, Clathrates, Chem. Rev. 59 (1959) 827–839.
[6] E.D. Sloan, C.A. Koh, Clathrate Hydrates of Natural Gases, third ed., CRC Press, 2007.
[7] S. Alavi, J.A. Ripmeester, D.D. Klug, Molecular-dynamics study of structure II hydrogen clathrates, J. Chem. Phys. 123 (2005) 024507(1)–024507(7).
[8] H.P. Veluswamy, R. Kumar, P. Linga, Hydrogen storage in clathrate hydrates: Current state of the art and future directions, Appl. Energy 122 (2014) 112–132.
[9] T.A. Strobel, K.C. Hester, C.A. Koh, A.K. Sum, E.D.S. Jr, Properties of the clathrates of hydrogen and developments in their applicability for hydrogen storage, J. Phys. Chem. Lett. 478 (2009) 97–109.
[10] C.J. Burnham, N.J. English, Free-Energy Calculations of the Intercage Hopping Barriers of Hydrogen Molecules in Clathrate Hydrates, J. Phys. Chem. C 120 (2016) 16561–16567.
[11] N.J. English, C.J. Burnham, Intra-Cage Structure, Vibrations and Tetrahedral-Site Hopping of H_2 and D_2 in Doubly-Occupied $5^{12}6^4$ Cages in sII Clathrate Hydrates from Path-Integral and Classical Molecular Dynamics, Appl. Sci. 11 (2021) 54(1)–54(9).
[12] J.R. Cendagorta, A. Powers, T.J.H. Hele, O. Marsalek, Z. Bacic, M.E. Tuckerman, Competing quantum effects in the free energy profiles and diffusion rates of hydrogen and deuterium molecules through clathrate hydrates, Phys. Chem. Chem. Phys. 18 (2016) 32169–32177.
[13] H. Itoh, J.S. Tse, K. Kawamura, The structure and dynamics of doubly occupied Ar hydrate, J. Chem. Phys. 115 (2001) 9414–9420.
[14] N.I. Papadimitriou, I.N. Tsimpanogiannis, A.K. Stubos, Computational approach to study hydrogen storage in clathrate hydrates, Colloids Surfaces A: Physicochem. Eng. Aspects 357 (2010) 67–73.
[15] S. Patchkovskii, J.S. Tse, Thermodynamic stability of hydrogen clathrates, PNAS 100 (2003) 14645–14650.
[16] E.P. van Klaveren, J.P.J. Michels, J.A. Schouten, D.D. Klug, J.S. Tse, Stability of doubly occupied N_2 clathrate hydrates investigated by molecular dynamics simulations, J. Chem. Phys. 114 (2001) 5745–5754.
[17] E.P. van Klaveren, J.P.J. Michels, J.A. Schouten, D.D. Klug, J.S. Tse, Molecular dynamics simulation study of the properties of doubly occupied N_2 clathrate hydrates, J. Chem. Phys. 115 (2001) 10500–10508.
[18] E.P. van Klaveren, J.P.J. Michels, J.A. Schouten, D.D. Klug, J.S. Tse, Computer simulations of the dynamics of doubly occupied N_2 clathrate hydrates, J. Chem. Phys. 117 (2002) 6637–6645.
[19] S. Alavi, J.A. Ripmeester, D.D. Klug, Molecular-dynamics simulations of binary structure II hydrogen and tetrahydrofurane clathrates, J. Chem. Phys. 124 (2006) 014704(1)–014704(6).
[20] A. Vidal-Vidal, M. Pérez-Rodríguez, M.M. Piñeiro, Direct transitions mechanism for molecular diffusion in gas hydrates, RSC Adv. 6 (2016) 1966–1972.
[21] M. Prager, J. Pieper, A. Buchsteiner, A. Desmedt, Methyl rotational potentials as a probe of the cage potential surface in methyl iodide clathrate, Phys. B: Condens. Matter 350 (2004) E399–E402.
[22] J.-H. Yoon, D. Lee, J.-W. Lee, Spectroscopic Identification on CO2 Separation from CH4 + CO2 Gas Mixtures Using Hydroquinone Clathrate Formation, Energies 14 (14), doi: 10.3390/en14144068, ISSN 1996-1073, https://www.mdpi.com/1996-1073/14/14/4068.
[23] S.C. Wallwork, H.M. Powell, The Crystal Structure of the α Form of Quinol, J. Chem. Soc., Perkin Trans. 2 (1980) (1980) 641–646.
[24] J.-H. Yoon, Y.-J. Lee, J. Park, T. Kawamura, Y. Yamamoto, T. Komai, S. Takeya, S.S. Han, J.-W. Lee, Y. Lee, Hydrogen Molecules Trapped in Interstitial Host Channels of α-hydroquinone, Chem. Phys. Chem. 10 (2009) 352–355.
[25] Y.A. Dyadin, I.V. Bondaryuk, L.S. Aladko, Stoichiometry of clathrates, J. Struct. Chem. 36 (1995) 995–1045.
[26] K. Maartmann-Moe, The Crystal Structure of γ-Hydroquinone, Acta Crystallogr. 21 (1966) 979–982.
[27] D.E. Palin, H.M. Powell, Hydrogen Bond Linking of Quinol Molecules, Nature 156 (1945) 334–335.
[28] D.E. Palin, H.M. Powell, The Structure of Molecular Compounds. Part III. Crystal Structure of Addition Complexes of Quinol with Certain Volatile Compounds, J. Chem. Soc. 1947 (1947) 208–221.
[29] D.E. Palin, H.M. Powell, The Structure of Molecular Compounds. Part VI. The β-Type Clathrate Compounds of Quinol, J. Chem. Soc. 1948 (1948) 815–821.
[30] V.F. Rozsa, T.A. Strobel, Triple Guest Occupancy and Negative Compressibility in Hydrogen-Loaded β-Hydroquinone Clathrate, J. Phys. Chem. Lett. 5 (2014) 1880–1884.
[31] J.-P. Torré, R. Coupan, M. Chabod, E. Pere, S. Labat, A. Khoukh, R. Brown, J.-M. Sotiropoulos, H. Gornitzka, CO_2-Hydroquinone Clathrate: Synthesis, Purification, Characterization and Crystal Structure, Cryst. Growth Des. 16 (2016) 5330–5338.
[32] R. Coupan, M. Chabod, C. Dicharry, J. Diaz, C. Miqueu, J.-P. Torré, Experimental Determination of Phase Equilibria and Occupancies for CO_2, CH_4, and N_2 Hydroquinone Clathrates, J. Chem. Eng. Data 61 (2016) 2565–2572.
[33] B.-S. Kim, Y. Lee, J.-H. Yoon, Pressure-Dependent Release of Guest Molecules and Structural Transitions in Hydroquinone Clathrate, J. Phys. Chem. B 117 (2013) 7621–7625.
[34] J.-W. Lee, S.J. Yoon, J.-H. Yoon, Selective Recovery of H_2S from Gas Mixtures Using a Hydroquinone Clathrate, J. Chem. Eng. Data 62 (2017) 2149–2154.
[35] S.J. Yoon, D. Lee, J.-H. Yoon, J.-W. Lee, Swapping and Enhancement of Guest Occupancies in Hydroquinone Clathrates Using CH_4 and CO_2, Energy Fuels 33 (2019) 6634–6640.
[36] Y. Woo, M. Pérez-Rodríguez, J.H. Jeong, M.M. Piñeiro, J.-W. Lee, Y. Lee, S.-H. Jung, H. Kim, S. Takeya, Y. Yamamoto, J.-H. Yoon, Extremely Slow Diffusion of Argon Atoms in Clathrate Cages: Implications for Gas Storage in Solid Materials, ACS Sustain. Chem. Eng. 9 (2021) 7479–7488.
[37] M.M. Conde, J.P. Torré, C. Miqueu, Revisiting the thermodynamic modelling of type I gas–hydroquinone clathrates, Phys. Chem. Chem. Phys. 18 (2016) 10018–10027.
[38] L.X. Dang, B.M. Pettitt, A theoretical study of the inclusion complexes of βquinol, J. Chem. Phys. 89 (1988) 968–974.
[39] L.X. Dang, B.M. Pettitt, Thermodynamics of Diatomic Guests in β-Quinol Clathrates, J. Phys. Chem. 93 (1989) 3794–3799.
[40] A. Comesaña, M. Pérez-Rodríguez, A.M. Fernández-Fernández, M.M. Piñeiro, A description of hydroquinone clathrates using molecular dynamics: Molecular model and crystalline structures for CH_4 and CO_2 guests, J. Chem. Phys. 148 (2018) 244502(1)–244502(9).
[41] E. Eikeland, M.K. Thomsen, J. Overgaard, M.A. Spackman, B.B. Iversen, Intermolecular Interaction Energies in Hydroquinone Clathrates at High Pressure, Cryst. Growth Des. 17 (2017) 3834–3846.
[42] A. Nemkevich, M.A. Spackman, B. Corry, Mechanism of Concerted Hydrogen Bond Reorientation in Clathrates of Dianin's Compound and Hydroquinone, J. Am. Chem. Soc. 133 (2011) 18880–18888.

[43] A. Nemkevich, B. Corry, M.A. Spackman, Computational study of methyl group dynamics in the hydroquinone clathrate of acetonitrile, Phys. Chem. Chem. Phys. 14 (2012) 1570–1572.
[44] A. Nemkevich, M.A. Spackman, B. Corry, Simulations of Guest Transport in Clathrates of Dianin's Compound and Hydroquinone, Chem. Eur. J. 19 (2013) 2676–2684.
[45] H.F. Clausen, M.R.V. Jørgensen, S. Cenedese, M.S. Schmøkel, M. Christensen, Y.-S. Chen, G. Koutsantonis, J. Overgaard, M.A. Spackman, B.B. Iversen, Host Perturbation in a β-Hydroquinone Clathrate Studied by Combined X-ray/Neutron Charge-Density Analysis: Implications for Molecular Inclusion in Supramolecular Entities, Chem. Eur. J. 20 (2014) 8089–8098.
[46] A. Grosjean, P.R. Spackman, A.J. Edwards, K. Tolborg, E.S. Vosegaard, G.A. Koutsantonis, B.B. Iversen, M.A. Spackman, Insights into Host-Guest Binding in Hydroquinone Clathrates: Single-Crystal X-ray and Neutron Diffraction, and Complementary Computational Studies on the Hydroquinone-CO_2 Clathrate, Cryst. Growth Des. 21 (2021) 3477–3486.
[47] K. Hermansson, Host–guest interactions in an organic crystal: β-hydroquinone clathrate with Ne and HF guests, J. Chem. Phys. 112 (2000) 835–840.
[48] P. Santikary, S. Yashonath, C.N.R. Rao, Molecular dynamics simulation of clathrates: noble gases in the cages of (β-hydroquinone, Chem. Phys. Lett. 192 (1992) 390–394.
[49] V.E. Zubkus, I.L. Shamovsky, E.E. Tornau, Computersimulation studies of βquinol clathrate with various gases. Molecular interactions and crystal structure, J. Chem. Phys. 97 (1992) 8617–8627.
[50] L. von Szentpály, I.L. Shamovsky, R. Ghosh, V.E. Zubkus, E.E. Tornau, Computer simulation studies on βquinol clathrates with various gases. Interdependence of host and guest molecules, J. Chem. Phys. 101 (1994) 683–692.
[51] V.E. Zubkus, I.L. Shamovsky, Molecular interactions, structure and stability of β-quinol clathrate, Chem. Phys. Lett. 195 (1992) 135–143.
[52] R. Coupan, E. Péré, C. Dicharry, F. Plantier, J. Diaz, A. Khoukh, J. Allouche, S. Labat, V. Pellerin, J.-P. Grenet, J.-M. Sotiropoulos, P. Senechal, F. Guerton, P. Moonen, J.-P. Torré, Characterization Study of CO_2, CH_4, and CO_2/ CH_4 Hydroquinone Clathrates Formed by Gas-Solid Reaction, J. Phys. Chem. C 121 (2017) 22883–22894.
[53] R. Coupan, E. Péré, C. Dicharry, J.-P. Torré, New Insights on Gas Hydroquinone Clathrates Using in Situ Raman Spectroscopy: Formation/Dissociation Mechanisms, Kinetics, and Capture Selectivity, J. Phys. Chem. A 121 (2017) 5450–5458.
[54] R. Coupan, M.M. Conde, C. Miqueu, C. Dicharry, J.-P. Torré, Phase Equilibrium Properties of CO_2/CH_4 Mixed Gas Hydroquinone Clathrates: Experimental Data and Model Predictions, J. Chem. Thermodyn. 116 (2018) 230–234.
[55] R. Coupan, C. Dicharry, J.-P. Torré, Hydroquinone clathrate based gas separation (HCBGS): Application to the CO_2/CH_4 gas mixture, Fuel 226 (2018) 137–147.
[56] J.-P. Torré, H. Gornitzka, R. Coupan, C. Dicharry, M. Pérez-Rodríguez, A. Comesaña, M.M. Piñeiro, Insights into the Crystal Structure and Clathration Selectivity of Organic Clathrates Formed with Hydroquinone and (CO_2 + CH_4) Gas Mixtures, J. Phys. Chem. C 123 (2019) 14582–14590.
[57] J.-W. Lee, J.-H. Yoon, Preferential Occupation of CO_2 Molecules in Hydroquinone Clathrates Formed from CO_2/N_2 Gas Mixtures, J. Phys. Chem. C 115 (2011) 22647–22651.
[58] Y.-J. Lee, K.W. Han, J.S. Jang, T.-I. Jeon, J. Park, T. Kawamura, Y. Yamamoto, T. Sugahara, T. Vogt, J.-W. Lee, Y. Lee, J.-H. Yoon, Selective CO_2 Trapping in Guest-Free Hydroquinone Clathrate Prepared by Gas-Phase Synthesis, Chem. Phys. Chem. 12 (2011) 1056–1059.
[59] J.-W. Lee, S.-P. Kang, J.-H. Yoon, Competing Occupation of Guest Molecules in Hydroquinone Clathrates Formed from Binary C_2H_4 and CH_4 Gas Mixtures, J. Phys. Chem. C 118 (2014) 7705–7709.
[60] J.-W. Lee, J. Poudel, M. Cha, S.J. Yoon, J.-H. Yoon, Highly Selective CO_2 Extraction from a Mixture of CO_2 and H_2 Gases Using Hydroquinone Clathrates, Energy Fuels 30 (2016) 7604–7609.
[61] J.-W. Lee, S.H. Lee, S.J. Yoon, J.-H. Yoon, Spectroscopic investigation, cage occupancy, and gas storage capacity of hydroquinone clathrates formed with H_2S-N_2 and COS-N_2 binary gas mixtures, Korean J. Chem. Eng. 34 (2017) 2710–2714.
[62] J.-W. Lee, S.H. Lee, S.J. Yoon, J.-H. Yoon, Spectroscopic Studies on the Formation and Guest Behaviors of Hydroquinone Clathrate with Binary CO and H_2 Gas Mixtures, Energy Fuels 32 (2018) 6863–6868.
[63] S.J. Yoon, D. Lee, J.-H. Yoon, J.-W. Lee, Guest Partitioning and High CO_2 Selectivity in Hydroquinone Clathrates Formed from Ternary (CO + CO_2 + H_2) Gas Mixtures, Energies 13 (2020) 3591(1)–3591(10).
[64] S.J. Yoon, D. Lee, J.-H. Yoon, J.-W. Lee, High Selectivity for CO_2 in Hydroquinone Clathrates Formed from Binary (CO + CO_2) Gas Mixtures with Various Compositions, Energy Fuels 35 (2021) 2478–2484.
[65] T.A. Strobel, Y. Kim, G.S. Andrews, J.R.F. III, C.A. Koh, A.M. Herring, E.D. Sloan, Chemical-Clathrate Hybrid Hydrogen Storage: Storage in Both Guest and Host, J. Am. Chem. Soc. 130 (2008) 14975–14977.
[66] K.W. Han, Y.-J. Lee, J.S. Jang, T.-I. Jeon, J. Park, T. Kawamura, Y. Yamamoto, T. Sugahara, T. Vogt, J.-W. Lee, Y. Lee, J.-H. Yoon, Fast and reversible hydrogen storage in channel cages of hydroquinone clathrate, Chem. Phys. Lett. 546 (2012) 120–124.
[67] J.L. Daschbach, T.-M. Chang, L.R. Corrales, L.X. Dang, P. McGrail, Molecular Mechanisms of Hydrogen-Loaded β-Hydroquinone Clathrate, J. Phys. Chem. B 110 (2006) 17291–17295.
[68] M. PérezRodríguez, J. Otero-Fernández, A. Comesaña, A.M. Fernández-Fernández, M.M. Piñeiro, Simulation of Capture and Release Processes of Hydrogen by β-Hydroquinone Clathrate, ACS Omega 3 (2018) 18771–18782.
[69] H. Bekker, H.J.C. Berendsen, E.J. Dijkstra, S. Achterop, R. van Drunen, D. van der Spoel, A. Sijbers, H.K. et al., Gromacs: A parallel computer for molecular dynamics simulations, Phys. Comput. 92 (1993) 252–256.
[70] D. van der Spoel, E. Lindahl, B. Hess, G. Groenhof, A.E. Mark, H.J.C. Berendsen, GROMACS: Fast, Flexible and Free, J. Comp. Chem. 26 (2005) 1701–1718.
[71] M.J. Abraham, T. Murtola, R. Schulz, S. Páll, J. Smith, B. Hess, E. Lindahl, GROMACS: High performance molecular simulations through multi-level parallelism from laptops to supercomputers, SoftwareX 1 (2015) 19–25.
[72] W.L- Jorgensen, D.S. Maxwell, J. Tirado-Rives, Development and testing of the OPLS all-atom force field on conformational energetics and properties of organic liquids, J. Am. Chem. Soc. 118 (45) (1996) 11225–11236.
[73] N. Michaud-Agrawal, E.J. Denning, T.B. Woolf, O. Beckstein, MDAnalysis: A Toolkit for the Analysis of Molecular Dynamics Simulations, J. Comput. Chem. 32 (2011) 2319–2327.
[74] R.J. Gowers, M. Linke, J. Barnoud, T.J.E. Reddy, M.N. Melo, S.L. Seyler, D.L. Dotson, J. Domanski, S. Buchoux, I.M. Kenney, O. Beckstein, MDAnalysis: A Python package for the rapid analysis of molecular dynamics simulations, in: Proceedings of the 15th Python in Science Conference, 2016, pp. 98–105.
[75] W.L. Jorgensen, T.B. Nguyen, Monte Carlo simulations of the hydration of substituted benzenes with OPLS potential functions, J. Comput. Chem. 14 (1993) 195–205.
[76] L. Martínez, R. Andrade, E.G. Birgin, J.M. Martínez, PACKMOL: a package for building initial configurations for molecular dynamics simulations, J. Comput. Chem. 30 (2009) 2157–2164.
[77] T. Darden, D. York, L. Pedersen, Particle mesh Ewald: An $N\,log(N)$ method for Ewald sums in large systems, J. Chem. Phys. 98 (1993) 10089–10094.
[78] R.J. Good, C.J. Hope, Test of Combining Rules for Intermolecular Distances. Potential Function Constants from Second Virial Coefficients, J. Chem. Phys. 55 (1971) 111–116.
[79] B. Hess, H. Bekker, H.J.C. Berendsen, J.G.E.M. Fraaije, LINCS: A linear constraint solver for molecular simulations, J. Comp. Chem. 18 (1997) 1463–1472.
[80] B. Hess, P-LINCS: A Parallel Linear Constraint Solver for Molecular Simulation, J. Chem. Theory Comp. 4 (2007) 116–122.
[81] G. Bussi, D. Donadio, M. Parrinello, Canonical sampling through velocity rescaling, J. Chem. Phys. 126 (2007) 014101(1)–014101(7).
[82] M. Parrinello, A. Rahman, Crystal Structure and Pair Potentials: A Molecular-Dynamics Study, Phys. Rev. Lett. 45 (1980) 1196–1199.
[83] M. Parrinello, A. Rahman, Polymorphic transitions in single crystals: A new molecular dynamics method, J. Appl. Phys. 52 (1981) 7182–7190.
[84] S. Plimpton, Fast Parallel Algorithms for Short-Range Molecular Dynamics, J. Comp. Phys. 117 (1995) 1–19.
[85] H. Tanaka, The thermodynamic stability of clathrate hydrate. III. Accommodation of nonspherical propane and ethane molecules, J. Chem. Phys. 101 (1994) 10833–10842.
[86] H. Tanaka, A novel approach to the stability of clathrate hydrates: grandcanonical MC simulation, Fluid Phase Equilib. 144 (1998) 361–368.
[87] D.-H. Chun, T.-Y. Lee, Molecular simulation of cage occupancy and selectivity of binary THF–H_2 sII hydrate, Mol. Sim. 34 (2008) 837–844.
[88] R.F. Cracknell, Molecular simulation of hydrogen adsorption in graphitic nanofibres, Phys. Chem. Chem. Phys. 3 (2001) 2091–2097.
[89] J.-P. Ryckaert, G. Ciccotti, H.J.C. Berendsen, Numerical integration of the cartesian equations of motion of a system with constraints: molecular dynamics of n-alkanes, J. Comp. Phys. 23 (1977) 327–341.
[90] W.G. Hoover, Canonical dynamics: equilibrium phase-space distributions, Phys. Rev. A 31 (1985) 1695–1697.